Proceedings of the 9th APTE Conference
6th - 8th August 2014, Mount Lavinia Hotel, Sri Lanka

NUMERICAL ANALYSIS OF HORN EFFECT REDUCTION ON POROUS PAVEMENT

Lei Zhang
Graduate Research Scholar
Dept. of Civil & Environmental Engineering
National University of Singapore
Singapore
Email: a0068326@nus.edu.sg

Ghim Ping Ong
Lecturer
Dept. of Civil & Environmental Engineering
National University of Singapore
Singapore
Email: ceeongr@nus.edu.sg

Tien Fang Fwa
Professor
Dept. of Civil & Environmental Engineering
National University of Singapore
Singapore
Email: ceefwatf@nus.edu.sg

ABSTRACT

Porous pavement is often seen as an effective engineering solution to reduce traffic noise. It works by reducing the horn effect of tire/road noise generation using its acoustic absorbing ability. Sound energy dissipates when it propagates through the porous surface layer due to the viscous and thermal effects resulting from the compression and expansion of air within the micro-structure of pore network. This sound absorption becomes more significant when it comes to horn effect because the multi-reflection process makes the absorption occur multiple times in sound propagation. Despite the significance of horn effect reduction on porous pavement, research studies on this topic are still limited to date. This paper attempts to investigate the horn effect reduction in a numerical perspective. A brief description of the acoustic characteristics of porous pavement is presented. Representative phenomenological and microstructural models which are capable to derive the acoustic impedance of porous pavement from its volumetric and composition characteristics are introduced. A numerical horn effect measurement model using boundary element method is then developed and validated against experimental results. This model is next used to analyze horn effect reduction on porous pavement. The influence of source position, the directivity of horn effect reduction, as well as the influence of the thickness and porosity of porous layer are examined. The simulation results demonstrate the feasibility of BEM model in the analysis of noise propagation on porous pavement and can provide some in-depth understanding of the horn effect on porous pavement.

Keywords: tire/road noise, horn effect, porous pavement, acoustic absorption, BEM model

1. INTRODUCTION

Noise generated from tire-pavement interaction has become a major component of traffic noise even at moderate speeds for modern vehicles as a result of the significant reduction in engine noise and aerodynamic noise (Sandberg and Ejsmont 2002). It is essential to develop engineering solutions to reduce the tire/road noise since it is responsible for a large proportion of environment pollution (Graf et al. 2002). A number of mechanisms are involved in the generation and propagation of tire/road noise. Their interactions and dependencies with each other make the problem complicated and difficult to be thoroughly understood. However, it has been identified that nearly all the noise sources (e.g. tire vibration, air pumping, stick-slip and acoustic resonance) exist near the tire-pavement contact patch, where a horn-shape geometry is formed by the tire tread and pavement surface. This horn-shape forces a multi-reflection of sound wave and thus causes a significant enlarging effect in its propagation. The sound amplification due to horn effect could be 10 to 20 dB (Kropp et al. 2000; Graf et al. 2002).

Porous asphalt surface is one of the most effective pavement technologies for noise reduction to date (Praticò and Anfosso-Lédée 2012). Porous mixture commonly utilizes uniform-size or open-graded aggregates and high-viscosity modified binders to form a skeleton with a porosity around 20%. Porous pavement behaves differently in the generation and propagation of tire/road noise, comparing to the conventional non-porous surfaces, resulting in a noise reduction of 3 to 5 dB (Bérengier et al. 1997). This is achieved mainly through two mechanisms (Neithalath et al. 2005): reduction in air pumping and depression in horn effect. The former happens when air is pumped out of or sucked into the gaps between tire tread and pavement by permitting air to escape through the interconnected pores within pavement layer. The later results from the absorption of sound energy in the multi-reflection process when sound wave propagates in the horn-shape geometry. This paper focuses on the second effect by analyzing the influence of porous surface layer on the reduction of horn amplification effect.

Experimental studies on horn effect have been conducted by various researchers, on both conventional pavements and porous surfaces. Graf et al. (2002) carried out noise measurements using a stationary loaded tire placed on a plane reflecting floor in an anechoic chamber. Reciprocal theorem was adopted to configure the test set-up, with a white noise source in far field and a microphone near the contact patch. Sound spectra with and without tire present were measured and their ratio was taken to denote the horn amplification. The horn effect was found to be significant, up to 20 dB for some frequencies. An interference pattern with distinct minima was observed at high frequencies. This study also found that the amplification function is independent of the longitudinal source position for low frequencies when source located close to the contact patch. These findings provided basic understandings of horn effect characteristics on conventional pavements. Similar measurements were conducted on porous pavements by Peeters et al. (2008; 2010) to investigate the effect of porous surfaces on noise radiation. The reciprocal theorem was also adopted in these tests, but the tire was unloaded and the source was placed at near field. A direct relationship between the acoustic properties of porous layer and the horn effect reduction was found. The peaks of noise reduction spectra were shifted to higher frequencies by a factor of about 1.2, with respect to the peaks of acoustic absorption spectra. The acoustic absorption around 2000 Hz and above was found less influential to the horn effect reduction. The measured horn effect reduction on porous pavement ranges up to 12 dB at the peak frequency around 1000 Hz.

Besides experimental studies, theoretical models were also developed to analyze the horn effect on porous pavement. Kuo et al. (2002) used the classic ray theory and compact body scattering model to study the horn effect at high and low frequencies, respectively. Although these approaches provided a useful physical basis for the interpretation of horn amplification, the ray theory was found agree well with experiments only for frequencies higher than 3000 Hz while the compact tire model only worked below 300 Hz. It was indicated that numerical model could be more effective to accurately predict the horn effect in the frequency range of practical interest (approximately 500 to 2500 Hz). Peeters and Kuijpers (2008) developed a mathematical model based on the extensive experimental measurements to predict the horn effect reduction on porous surface, with acoustic absorption spectrum serving as an input of the model. It took into account the frequency shift between noise reduction peak and effective absorption coefficient for multiple reflections. Lui and Li (2004) proposed a simplified theoretical model based on the sound diffracted by a sphere to investigate the horn effect on porous pavement, with a monopole source located on tire tread surface. The effectiveness of porous pavement on horn effect reduction was proved in the parametric study. An increase in the thickness and porosity of the porous layer was found to further attenuate the horn amplification. The horn effect on porous surface was demonstrated to be less dependent on the air flow resistance of pavement course and the angular position of noise source.

Despite of the significance of porous pavement on the reduction in horn amplification of tire/road noise, the research studies on this topic is still quite limited and the understanding of the phenomenon is far from satisfaction. This paper attempts to approach this problem in a numerical perspective. A 3D boundary element method (BEM) model is developed based on the stationary-tire test configuration. The sound field is computed with a monopole source placed near the tire-pavement contact patch. The

acoustic property of porous pavement is represented by the complex acoustic impedance, which could be theoretically derived from the volumetric parameters of porous surface layer and serves as a critical input in the BEM model. After being validated against published experiment data, the model is then used to analyze the characteristics of horn effect reduction on porous pavement.

2. ACOUSTIC PROPERTY OF POROUS PAVEMENT

Porous pavement is a rigid-frame porous media, whose pore walls do not deform with the air pressure fluctuation within the pores. Acoustic wave propagates in rigid-frame porous media by alternating air compression and expansion. In this process, acoustic absorption occurs as a result of energy losses due to viscous effect and thermo-elastic damping (Neithalath et al. 2005). The sound propagation in porous pavement is governed by the effective density and effective bulk modulus of the air within the pores (Brennan and To 2001). These quantities are frequency-dependent, complex and non-linear. Acoustic absorption coefficient is a fundamental intuitive parameter commonly used to describe the ability of a material absorbing and transmitting sound energy when sound waves collide with it. It is defined as:

$$\alpha = I_a / I_i \tag{1}$$

where α is the acoustic absorption coefficient, I_a is the sound intensity absorbed, and I_i is the incident sound intensity. The fraction of sound absorbed is governed by the acoustic impedance of a porous pavement, which indicates the amount of sound pressure generated by the molecule vibrations of an acoustic medium at a given frequency. The specific impedance (Z) is defied as the ratio of sound pressure to the particle velocity at the surface of porous material. A phase difference generally exists between the pressure and the particle velocity. Therefore, the specific acoustic impedance is usually expressed as a complex number:

$$Z = R + jM \tag{2}$$

where R is the real component of the impedance, representing the resistive part, M is the imaginary component, indicating the reactive part and j is the imaginary unit. The acoustic absorption coefficient can be theoretically related to the complex acoustic impedance by

$$\alpha = \frac{4R}{(R+1)^2 + M^2} \tag{3}$$

In practice, the porous pavement acoustic properties are usually measured by the sealed tube approach (ASTM 2012) in the lab, or through the extended surface method (ISO 2002) in the field. Moreover, various models have been developed to relate the acoustic property of porous mixture to its volumetric and composition characteristics (Hamet and Bérengier 1993; Hubelt 2003; Neithalath et al. 2005; Kim and Lee 2010). The availability of variables usually determines which model should be adopted. This paper adopts the microstructural model developed by Neithalath et al. (2005), which relates acoustic absorption of porous pavement to its porosity, characteristic pore size and porous layer thickness.

Recognizing the fact that air is alternatively compressed and expanded when acoustic waves propagate through the porous mixture, Neithalath's model simplifies the pore network as a series of alternating cylinders with varying diameter (*see* Figure 1). Each unit of the pore structure consists of a pore (with diameter D_p and length L_p) and an aperture (with diameter D_a and length L_a). The porosity (ϕ) can be easily related to the pore structure dimensions and wall thickness (d) as:

$$\phi = \frac{D_a^2 L_a + D_p^2 L_p}{(L_a + L_p)(D_p + d)^2} \tag{4}$$

The characteristic pore size (D_p) is chosen as the median of all pore sizes greater than 1 mm, and can be obtained from image analysis. The other parameters are related to the pore size and porosity, and can be determined from an iterative process or an optimization algorithm (Losa and Leandri 2012). Porosity is maintained consistent in the simplification. The network is next modeled using an electro-acoustic analogy consisting of a series of resistors and inductors (*see* Figure 1). The air impedance in the pores (Z_p) is modeled by an inductor, the value of which is a function of the pore diameter:

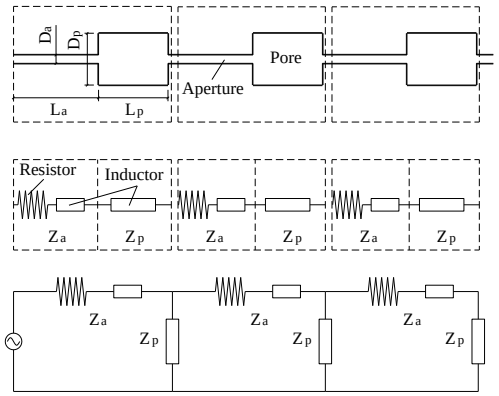

Figure 1: Electro-Acoustic Representation of Pore Structure

$$Z_p = -j \cdot \rho_{air} \cdot c \cdot \cot(\omega D_p / c) \tag{5}$$

The acoustic impedance of apertures (Z_a) is modeled by a resister and an inductor, representing the real component (R_a) and imaginary component (M_a) of the acoustic impedance, respectively.

$$Z_a = R_a + j \cdot M_a \tag{6}$$

$$R_a = \frac{32\eta L_a}{D_a^2} \cdot \left(\sqrt{1 + \frac{\beta^2}{32}} + \sqrt{\frac{\beta D_a}{4L_a}} \right) \tag{7}$$

$$M_a = \omega \rho_{air} L_a \cdot \left(1 + \frac{1}{\sqrt{9 + \beta^2/2}} + \frac{8D_a}{3\pi L_a} \right) \tag{8}$$

where η is the dynamic viscosity of air, and β is the acoustic Reynolds number. For a porous layer composed by n cells, the acoustic impedance is determined by applying the electro-acoustic analogy to all the cells and calculated using the following iterative relationship:

$$Z_n = Z_a \cdot \frac{D_p^2}{D_a^2} + \frac{1}{1/Z_p + 1/Z_{n-1}} \tag{9}$$

In above calculations, the air density (ρ_{air}) has been multiplied by a structure factor (k_s) to take into account the fact that all the pores do not contribute equally in sound absorption.

$$k_s = \frac{(L_a D_a^2 + L_p D_p^2) \cdot (L_a D_p^2 + L_p D_a^2)}{(L_a + L_p)^2 D_a^2 D_p^2} \tag{10}$$

This model has been validated against experimental measurements (Neithalath et al. 2005) and was applied on the analysis of acoustic characteristics of porous pavements (Losa and Leandri 2012).

3. BEM MODEL OF HORN EFFECT ON POROUS PAVEMENT

Boundary element method is next used to simulate the sound propagation on porous pavement and the amplification effect resulting from the horn-shape between tire tread and pavement surface. BEM is formulated in a way that integral equations are defined on the domain boundaries and an integration relates the boundary solutions to the field solutions. The sound pressure field is determined as long as the magnitude and gradient of pressure are known over the whole boundary. The integral form of Helmholtz equation on boundary relates boundary pressure and normal velocity by a matrix equation:

$$[A]\{p\} = [B]\{v_n\} \tag{11}$$

where [*A*] and [*B*] are coefficient matrices. Boundary conditions are applied to calculate the pressures and particle velocities at the boundaries. The acoustic pressure at any field point is next solved through the integration of boundary solutions:

$$p(x_f) = \{C\}^T \{p\} + \{D\}^T \{v_n\} \tag{12}$$

where {*C*} and {*D*} are coefficient vectors derived from the integration of Helmholtz equation.

Porous pavement is simulated by an absorbent panel in the BEM model, on which acoustic impedance is defined to represent its absorption properties. For the space above pavement surface, air at 25°C is modeled as the sound propagating medium. The mass density of air is set to be 1.225 kg/m^3 and the sound velocity in it is 340 m/s. Tire walls are modeled by perfectly reflecting panels based on the tire geometry used in the test, and monopole with white noise is used as sound source in the simulations. With such a configuration, the sound pressure field around the horn-shape is computed by the model.

The 3D BEM model is next validated against experimental results. The validation work is based on the differences between sound pressure levels on porous and non-porous pavements. The comprehensive measurements conducted by Schwanen et al. (2007) are used to validate the developed model because of its clearly defined test conditions and various tested scenarios. The experiment set-up is sketched in Figure 2. A tire of 195 mm width, 381 mm rim diameter and 310 mm outer radius is located on the measured pavement without vertical loading. Two source positions are selected on the center line of tire tread, 10 and 15 cm away from the center of contact patch, respectively. Two receiver positions are defined at the coordinates shown in Figure 2. Receiver A is right in front of the contact patch, 428 mm from its center. Receiver B is perpendicular to the tire center plane, at a distance of 297.5 mm. Both receivers are 100 mm above pavement surface. Two porous pavements and one conventional pavement are involved in the model validation work. The acoustic impedance of tested pavements is measured by the extended surface method (ISO 2002) and the results are shown in Figure 3. To isolate the influence of pavement absorption and eliminate the affects of tire tread material and groove pattern, a fully reflective wooden mock-up with the same geometry and a smooth tread surface is used in the measurement instead of a rubber tire. Such configuration makes the model validation more reliable.

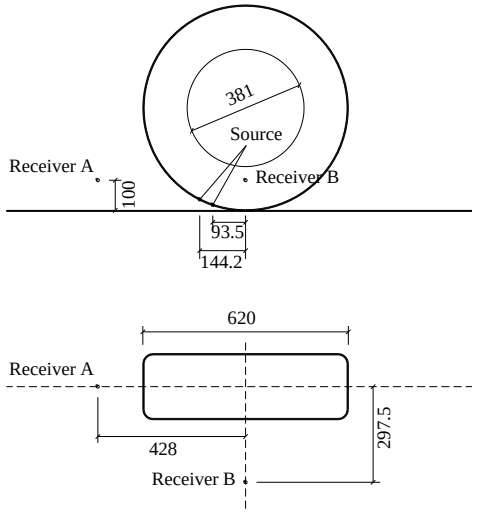

Figure 2. Experiment Set-up for Model Validation

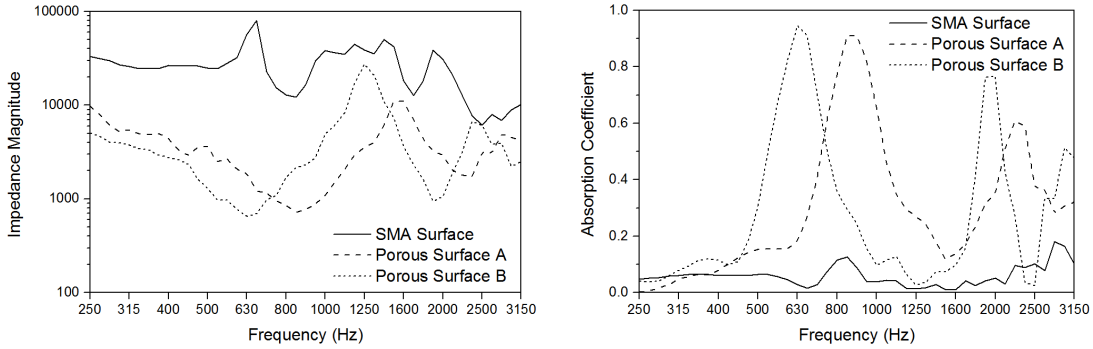

(a) Acoustic Impedance (b) Acoustic Absorption

Figure 3: Measured Acoustic Properties of Tested Pavements

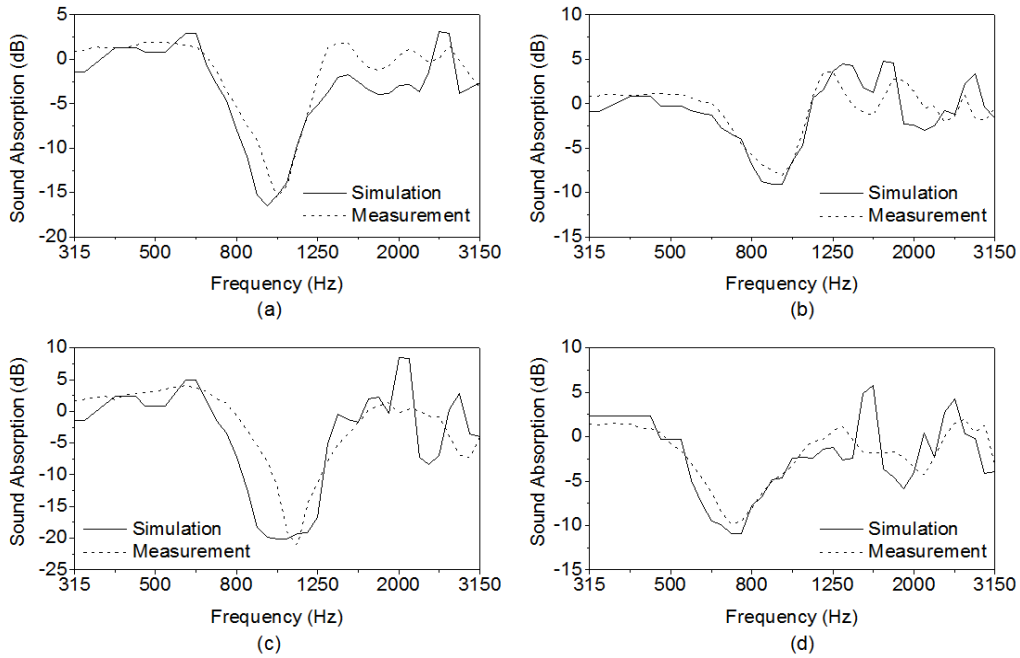

Figure 4: Model Validation Results

(a) Porous Surface A, Receiver A, and source is 10 cm from the center;
(b) Porous Surface A, Receiver A, and source is 15 cm from the center;
(c) Porous Surface A, Receiver B, and source is 10 cm from the center;

(d) Porous Surface B, Receiver A, and source is 10 cm from the center.

The effect of porous pavement on sound absorption is represented by the differences in sound pressure levels on porous and SMA surfaces. The results computed from numerical simulations are compared with the values measured in experiments (see Figure 4). Validations are conducted for different source positions, receiver locations and porous surfaces to better illustrate the feasibility and capability of the simulation model. It is seen that the BEM model is capable to predict the major peak frequency of sound absorption on porous pavement, as well as the magnitude of noise reduction at this frequency. However, the peak frequency range detected by receiver B in simulation is wider than that obtained in field measurement. This may due to the experiment set-up configuration. Besides, it is observed that the errors at high frequencies are larger than those at low frequencies and the prediction of secondary absorption peak is bellow satisfaction. Recognizing the fact that the differences between numerical and experimental results shown in Figure 4 include the errors in acoustic impedance measurements, wood mock-up geometry as well as sound pressure measurements, the accuracy of developed BEM model is considered to be good enough for engineering applications.

4. CHARACTERISTICS OF HORN EFFECT REDUCTION ON POROUS PAVEMENT

The developed BEM model is next used to analyze the characteristics and crucial influential factors of horn effect reduction on porous pavement. The factors involved in the analysis include the position of monopole source, the directivity of noise reduction, as well as the porosity and thickness of porous surface layer. The same tire geometry in the model validation is adopted in the analysis and perfectly reflecting tire surface condition is assumed. The simulated noise level on the SMA surface is used as comparison baseline for the horn effect reduction.

4.1 Influence of Source Position

Tire-pavement noise is generated by various sources from rolling tire vibration, pavement friction, air pumping and resonations. Almost all these sources locate near the tire-pavement contact patch, within the horn-shape geometry. The influence of longitudinal and lateral position of the monopole source is examined in this section. For longitudinal position, source is located on the middle line of tire tread, with a curved distance of 5, 10, 15 and 20 cm from the center point of tire-pavement contact patch. For literal position, source is placed on tire tread at the same distance of 10 cm from contact patch center, with a literal offset of 0, 3, 6 and 9 cm from the middle line of tire tread. Sound propagation on Porous Surface A (see Figure 3) is simulated by the BEM model and the reduction of sound pressure level at Receiver A (see Figure 2) with regards to that on the SMA surface is shown in Figure 5.

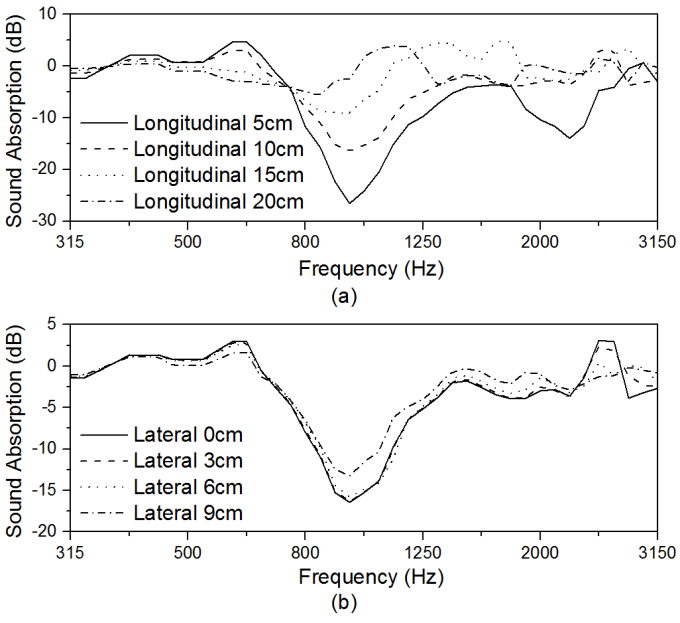

Figure 5: Influence of Source Position on Sound Absorption

Figure 5 (a) compares the noise reduction effects when the source move along the center line of tire tread. It is obvious that the longitudinal position of source has a significant influence on the sound absorption efficiency. When the source moves closer to the contact patch center, the peak value of sound absorption increases dramatically and the range of the high-efficiency frequency becomes wider. The first absorption peak shifts slightly towards higher frequency with the reduction in source distance and a second absorption peak is observed in the interested frequency range when the source is 5 cm away from the contact center. On the other hand, when the source is 20 cm away from the contact center, the sound absorption efficiency of porous pavement is found to be very low. With regards to the overall noise level reduction, 6.0 dB is obtained when the source is 5 cm from the contact center and 1.3 dB for the 20 cm case. It is concluded that the reduction in horn effect on porous pavement is more effective and efficient when the source is nearer to the contact patch, because in such cases more incidences of reflections may occur when sound propagates through the horn-shape geometry.

Figure 5 (b) shows the comparisons among various lateral positions while an identical distance of 10 cm is maintained between the source and contact center. The difference is marginal in the cases of 0, 3 and 6 cm, while the sound absorption efficiency at peak frequency becomes lower when the source is located 9 cm away from the middle line of tire tread. This is not unexpected because 9 cm is close to the edge of tire tread (i.e. tire shoulder) where the sound wave may not be fully reflected. The sound absorption curves possess similar shapes and peak at the same frequency for all the lateral positions examined. The reduction in overall noise level is 3.6 dB for the centered source position and 2.4 dB for the 9 cm offset case. Obviously, the influence of lateral position of source on horn effect reduction is not as significant as that of the longitudinal position.

4.2 Directivity of Horn Effect Reduction on Porous Pavement

Propagation of sound in directions other than the vehicle heading direction is more responsible for annoying residents along the roadway. Therefore, knowledge in the directivity of horn effect reduction is essential to evaluate the effectiveness of porous pavement on traffic noise mitigation. This effect is investigated by locating more receivers around the stationary tire to detect the sound pressure level at different directions. Besides the previously mentioned receiver locations (Receiver A and B), another seven microphones are placed in an array shown in Figure 6. The coordinates of all these receivers are given in Table 1. The monopole source is located on the center line of tire tread with 10 cm distance from the contact center. Simulations are conducted on both SMA surface and Porous Surface A (see Figure 3), and the sound level differences between the two pavements are shown in Figure 7.

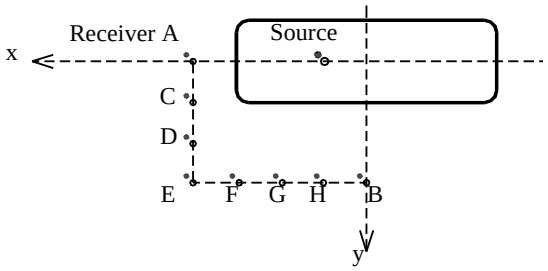

Figure 6: Schematic Diagram of Receiver Positions

It is seen that noise reduction curves for receivers with the same *x* value in front of the tire (Receiver C, D and E,) are very close to each other. The major peak frequencies concentrate at around 1000 Hz and the peak absorption are about 17 dB without significant differences among receiver positions. For the receivers with the same *y* value besides the tire (Receiver F, G and H), although the curve shapes are kept similar, the peak values of sound absorption are significantly different from one to another. The peak absorption increases with the attenuation of *x* value (i.e. receiver moves to the *y* axis). Large

differences among various receiver positions are observed at higher frequencies. However, due to the small magnitude of sound absorption in this range, the diversities are less important to this study. The observations are in consistent with the experimental findings obtained by Schwanen et al. (2007).

Table 1: Coordinates of Receiver Positions

Receiver Name	x (mm)	y (mm)	z (mm)
A	428	0	100
B	0	297.5	100
C	428	100	100
D	428	200	100
E	428	297.5	100
F	300	297.5	100
G	200	297.5	100
H	100	297.5	100

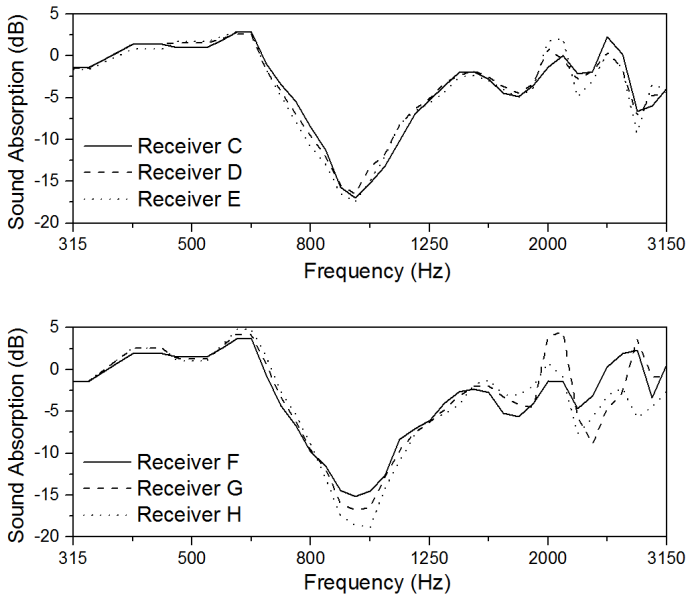

Figure 7: Directivity of Noise Reduction on Porous Pavement

4.3 Influence of Porous Layer Thickness

The thickness and porosity of porous surface layer are two essential parameters in porous pavement design. Previous experimental studies have shown that the peak frequency of acoustic absorption depends on the thickness of porous layer, while the magnitude of absorption coefficient is closely related to its porosity (Abbott et al. 2010). This section studies the influence of porous layer thickness on horn effect reduction using the simulation model, while the porosity influence is analyzed later.

To isolate the sole difference in porous layer thickness, Neithalath's microstructure model is used to derive the acoustic impedance of various porous surfaces with the identical porosity value of 20%. In practice, porous layers are commonly compacted into thickness of 50 to 100 mm, with some extremely thin lift of 25 mm occasionally used. Therefore, four thickness levels are examined in this work, which are 25, 50, 75 and 100 mm, respectively. The characteristic pore size (D_p) is assumed to be 4 mm. In an experimental study conducted by Losa and Leandri (2012), regression relationship between the pore length and pore size is developed as

$$L_p = 1.92 \cdot D_p + 6.08 \quad (13)$$

The pore length (L_p) is thus calculated to be 16.3 mm. In order to adapt to the tested layer thicknesses, the overall length of a pore unit is assumed to be 25 mm, which provides the length of aperture (L_a) to be 8.7 mm. The aperture diameter (D_a) is taken as a quarter of the pore size according to Neithalath's suggestion (Neithalath 2005). The pore wall thickness (d) is derived as 3.34 mm to maintain a porosity of 20%. With the above pore structure parameters, the acoustic impedance and absorption coefficient are derived based on Equation (3) to (10). The resulted acoustic absorption coefficients are shown in Figure 8(a). The primary absorption peak moves towards lower frequency with the increase in porous layer thickness and its magnitude is slightly higher on thicker porous layer. For 75 and 100 mm cases, a secondary absorption peak could be observed in the interested frequency range.

The acoustic impedances obtained from Neithalath's microstructure model are then input into the horn effect simulation model as the acoustic property of porous pavement. The source is fixed 10 cm away from the center of contact patch on the middle line of tire tread and the sound levels at Receiver A are computed from the BEM model. The results are then subtracted by the noise levels detected on the SMA surface in the same test configuration and the differences are shown in Figure 8(b). It is obvious that the peak frequencies of horn effect reduction on porous pavements correspond to the peaks of acoustic absorption coefficient. The noise reduction peak moves towards lower frequencies with the increase in porous layer thickness, but its magnitude becomes smaller. None of the tested pavements can significantly reduce the horn effect below 500 Hz, which may due to the large difference between porous layer thickness and sound wavelength at low frequency. It is also found that the secondary absorption peak does not have much influence on the noise reduction performance. The simulation results show the possibility of altering porous layer thickness to adjust the peak absorption frequency and make it more efficient according to the tire/road noise characteristics.

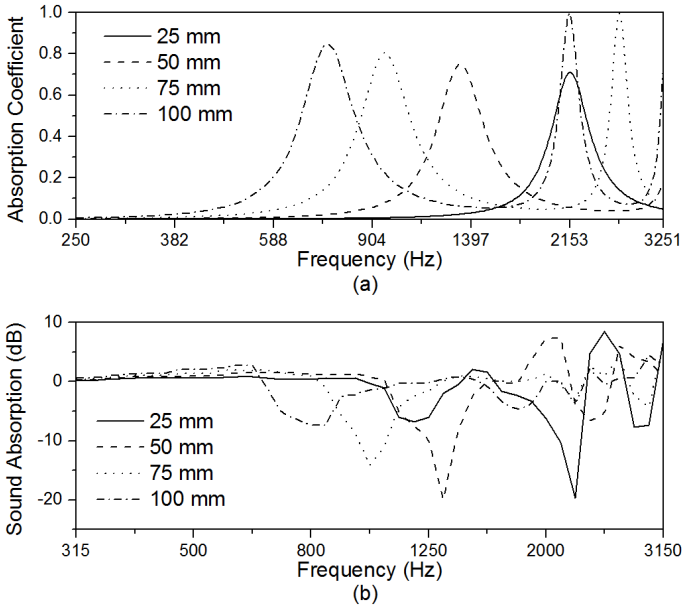

Figure 8: Absorption Coefficient and Horn Effect Reduction of Porous Pavements with 20% Porosity and Various Porous Layer Thicknesses

4.4 Influence of Porosity

The same method is used to analyze the influence of porous layer porosity on the horn effect reduction. Four porosity levels (i.e. 15%, 20%, 25% and 30%) are examined in this study. Since the characteristic pore size is closely related to the porosity, fixed pore size approach is inadequate in this part of work.

The pore size has to be tried out for each porosity value with relationships between pore size and other parameters (i.e. pore length, aperture length and aperture diameter). In the calculation, the thickness of pore wall is fixed at 3.34 mm. The pore size turns out to be 3.24, 4.00, 4.74 and 5.46 mm for the four porosity levels respectively. The acoustic absorption coefficients derived from Neithalath's model are shown in Figure 9(a). It is seen that porosity value does not have a significant influence on the peak absorption frequency, but it does affect the magnitude of peak absorption coefficient. In the examined porosity range, the peak value of acoustic absorption coefficient decreases with an increase of porosity. This is mainly due to the decrease in the real component of acoustic impedance, which represents the resistive part of energy lost.

BEM simulations are conducted with the derived acoustic impedances. The same test configuration as used in the previous subsection is adopted. The results of horn effect reductions on porous pavements with various porosities are shown in Figure 9(b). It is seen that the noise reduction curves have similar shapes over the whole interested frequency range, with peaks at nearly the same frequency. However, the magnitude of horn effect reduction at the peak frequency significantly increases with the increase in porosity value. This result indicates that porous pavement with larger porosity is desired to more efficiently reduce the tire/road noise level.

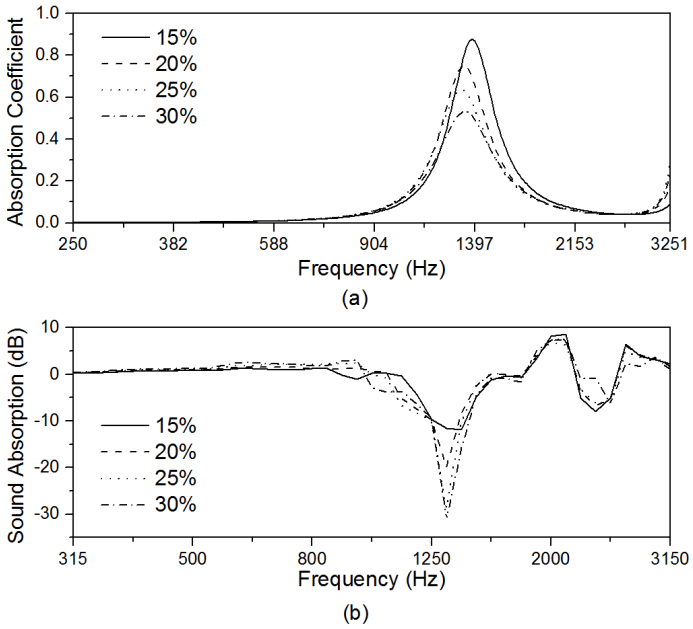

Figure 9: Absorption Coefficient and Horn Effect Reduction of Porous Pavement with 50 mm Porous Layer Thickness and Different Porosities

5. CONCLUSION

This paper implements a numerical model to analyze the reduction of horn effect on porous pavements. The complex acoustic impedance serves as an essential parameter describing the acoustic absorption properties of porous pavement surface. A representative microstructural model is first introduced to derive acoustic impedance from the volumetric and composition characteristics of porous surface layer. The BEM model is next developed based on the horn effect test configuration and is validated against published experimental data. The model is then used to analyze horn effect reduction on porous pavement. The following conclusions can be drawn from the analyses presented in the paper:

- Longitudinal source position has a significant influence on the horn effect reduction on porous pavement. Noise reduction is more efficient if the source is located nearer to the tire-pavement contact patch.

- Lateral position marginally affect the horn effect reduction unless the source is located at tire shoulder, in which the peak absorption is reduced.
- The noise reduction levels detected at different receiver positions vary as well, illustrating the directivity of the horn amplification. The reduction is found more obvious when the receiver is located at the side of the tire.
- With the increase in porous layer thickness, the peak of horn effect reduction moves to lower frequency and its amplitude attenuates.
- The variations in porosity do not influence the peak absorption frequency, but when larger porosity is provided, the magnitude of noise reduction peak increases.

Based on the model validation and case studies demonstrated in this paper, it is concluded that the representation of porous pavement acoustic property using acoustic impedance in the BEM model is valid and feasible. It is recommended to apply this approach on the rolling tire noise prediction and traffic noise analysis on porous pavement and assist in the porous surface layer design.

6. REFERENCES

Abbott, P.G., Morgan, P.A. and McKell, B., 2010. *A Review of Current Research on Road Surface Noise Reduction Techniques*, Transport Research Laboratory, Wokingham, UK.

ASTM, 2012. *Standard Test Method for Impedance and Absorption of Acoustical Materials Using a Tube, Two Microphones and a Digital Frequency Analysis System*. ASTM Standard E1050-12, ASTM International, West Conshohochen, Pennsylvania.

Bérengier, M.C., Stinson, M.R., Daigle, G.A. and Hamet, J.F., 1997. *Porous Road Pavements: Acoustical Characterization and Propagation Effects*. The Journal of the Acoustical Society of America, 101(1).

Brennan, M.J. and To, W.M., 2001. *Acoustic Properties of Rigid-Frame Porous Materials - An Engineering Perspective*. Applied Acoustics, 62(7), 793-811.

Graf, R.A.G., Kuo, C.Y., Dowling, A.P. and Graham, W.R., 2002. *On the Horn Effect of a Tyre/Road Interface, Part I: Experiment and Computation*. Journal of Sound and Vibration 256(3): 417-431.

Hamet, J.F. and Bérengier M.C., 1993. *Acoustical Characteristics of Porous Pavements: A New Phenomenological Model*. Internoise 93, Leuven, Belgium.

Hubelt, J., 2003. *Modeling of Porous Asphalt as Extended Reacting Absorber Using the Transmission-Line-Matrix-Method (TLM)*. Euronoise 2003, Naples, Italy.

ISO, 2002. *Acoustics - Measurement of Sound Absorption Properties of Road Surfaces in Situ - Part 1: Extended Surface Method*. ISO 13472-1, International Organization for Standardization, Geneva, Switzerland.

ISO, 2010. *Acoustics - Measurement of Sound Absorption Properties of Road Surfaces in Situ - Part 2: Spot Method for Reflective Surfaces*. ISO 13472-2, International Organization for Standardization, Geneva, Switzerland.

Lui, K.W. and Li, K.M., 2004. *A Theoretical Study for the Propagation of Rolling Noise over a Porous Road Pavement*. The Journal of the Acoustical Society of America, 116(1).

Kim, H.K. and Lee, H.K., 2010. *Acoustic Absorption Modeling of Porous Concrete Considering the Gradation and Shape of Aggregates and Void Ratio*. Journal of Sound and Vibration, 329(7), 866-879.

Kropp, W., Bécot, F.X. and Barrelet, S., 2000. *On the Sound Radiation From Tyres*. Acta Acoustica, 86(5), 769-779.

Kuo, C.Y., Graf, R.A.G., Dowling, A.P. and Graham, W.R., 2002. *On the Horn Effect of a Tyre/Road Interface, Part II: Asymptotic Theories*. Journal of Sound and Vibration, 256(3), 433-445.

Losa, M. and Leandri, P., 2012. *A Comprehensive Model to Predict Acoustic Absorption Factor of Porous Mixes*. Materials and Structures, 45(6), 923-940.

Neithalath, N., Marolf, A., Weiss, J. and Olek, J., 2005. *Modeling the Influence of Pore Structure on the Acoustic Absorption of Enhanced Porosity Concrete*. Journal of Advanced Concrete Technology, 3(1), 29-40.

Peeters, B., Ammerlaan, I., Kuijpers, A. and van Blokland, G., 2010. *Reduction of the Horn Effect for Car and Truck Tyres by Sound Absorbing Road Surfaces*. Internoise 2010, Lisbon, Portugal.

Peeters, B. and Kuijpers, A., 2008. *The Effect of Porous Road Surfaces on Radiation and Propagation of Tyre Noise*. The Journal of the Acoustical Society of America, 123(5).

Praticò, F.G. and Anfosso-Lédée, F., 2012. *Trends and Issues in Mitigating Traffic Noise through Quiet Pavements*. Procedia - Social and Behavioral Sciences, 53, 203-212.

Sandberg, U. and Ejsmont, J.A., 2002. *Tyre/Road Noise Reference Book*. INFORMEX, Kisa, Sweden.

Schwanen,W., van Leeuwen, H.M., Peeters, A.A.A., van Blokland, G.J., Reinink, H.F. and Kropp, W., 2007. *Acoustic Optimization Tool RE3: Measurement Data Kloosterzande Test Track*. Delft, The Netherlands.